Implantation of Pt_3^- and Ag_3^- clusters into graphite: an STM study

2001 J. Phys.: Condens. Matter 13 1869

(http://iopscience.iop.org/0953-8984/13/9/310)

INSTITUTE OF PHYSICS PUBLISHING JOURNAL OF PHYSICS: CONDENSED MATTER

J. Phys.: Condens. Matter **13** (2001) 1869–1872 www.iop.org/Journals/cm PII: S0953-8984(01)17750-7

Implantation of Pt_3^- and Ag_3^- clusters into graphite: an STM study

C-M Grimaud and R E Palmer

Nanoscale Physics Research Laboratory, School of Physics and Astronomy, The University of Birmingham, Edgbaston, Birmingham B15 2TT, UK

E-mail: r.e.palmer@bham.ac.uk

Received 4 October 2000, in final form 15 January 2001

Abstract

We have investigated the impact of small platinum clusters, Pt_3^-, on the surface of graphite for incident cluster energies in the range 50–1500 eV. The density of features observed in the STM rises markedly with increasing impact energy. Results for Pt_3^- clusters and the lighter Ag_3^- clusters can be overlaid, i.e. the feature density is independent of the cluster mass. This behaviour violates the binary elastic collision model for energy transfer to the substrate, but is consistent with recent simulations of the implantation of large clusters into the graphite surface.

(Some figures in this article are in colour only in the electronic version; see `www.iop.org`)

The deposition of clusters onto surfaces is motivated by several factors including (i) the production of thin films with properties not accessible via the deposition of atoms [1] and (ii) fundamental interest in the cluster–surface interaction. Several parameters such as the cluster size, the incident energy and the cohesive energies of both the cluster and the substrate determine the fate of the cluster [2]. The graphite surface has become a model for our developing understanding of cluster deposition [3–6]. Both experimental studies [7–11] and molecular dynamics simulations [12–16] have attempted to extend the existing body of data concerning atomic ion impact to cluster ion impact on graphite. For example, Carroll *et al* [13] have recently shown that the threshold energy for pinning of Ag_N^+ clusters to the surface, where $N = 50$–200, scales linearly with the cluster mass over the energy range 250–2500 eV. By contrast, the implantation depth (D) obtained from molecular dynamics simulations of the implantation of similar size Ag clusters ($N = 20$–200 atoms) at higher energies E, (0.75–6 keV) was not dependent explicitly on cluster mass i.e. on the size N [12]. In this study we compare the impact of Pt_3^- clusters on graphite with that of Ag_3^- clusters, in order to investigate the effect of the cluster mass on the impact of small energetic metal clusters on the graphite surface. We use scanning tunnelling microscopy to image the resulting surface after impact over a wide range of kinetic energies (from 50 eV to 1.5 keV).

Platinum and silver clusters were produced with a home built cluster source based on the principle of sputtering by positive caesium ions [17]. The source produces a beam of small cluster anions which is extracted at 1.5 kV and mass-selected by a Wien filter. Platinum

trimers were deposited at room temperature onto samples of highly oriented pyrolitic graphite (10×5 mm^2, ZYB grade from Advanced Ceramics). Prior to deposition, the graphite substrates were cleaved in air and placed in vacuum no longer than 30 minutes later. The samples were cleaned by heating to 150 °C in high vacuum (typical pressure between 5×10^{-7} and 10^{-6} mbar), for a couple of minutes by electron bombardment. We found that higher temperatures would lead to surface damage to the surface of the graphite samples ('bubbling'). Possibly this is due to the presence of some trapped gas near the surface. The samples were allowed to cool down to room temperature before cluster deposition in a pressure of 1×10^{-7} mbar. The energy of the incident clusters was controlled by applying a negative bias to the sample. The clusters impinged onto the surface with energies ranging from 50 eV to 1.5 keV. Typical currents on the samples during deposition were hundreds of pA and the dose of Pt_3^- clusters was of the order of 1–100 $\times$ 10^{12} cluster ions per cm^2. After deposition the surface was examined in air with a bench-top scanning tunnelling microscope (DME Rasterscope 4000). Typical values of the tip bias was 0.25 V. Cells of size 50×50 nm^2 were defined at different sites in the central region of each sample and the number of features in the image was counted. We counted hundreds of features at various locations on each sample to ensure reliable statistics.

The STM images immediately reveal that the density of features on the surface increases

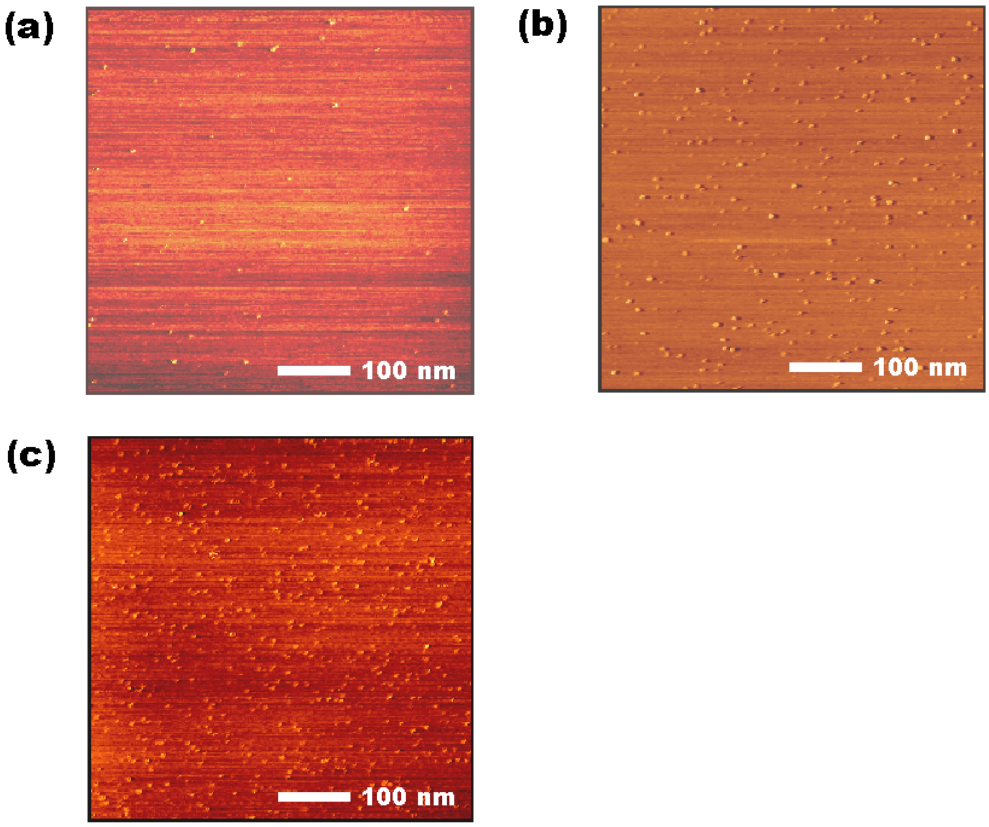

Figure 1. STM images of graphite after exposure to the same dose ($\sim 0.8 \times 10^{12}$ atoms cm^{-2}) of Pt_3^- clusters with different incident energies: (a) 25 eV ($I = 1.15$ nA, $V = 0.35$ V), (b) 250 eV ($I = 0.57$ nA, $V = 0.35$ V), (c) 1 keV ($I = 1.15$ nA, $V = 0.35$ V).

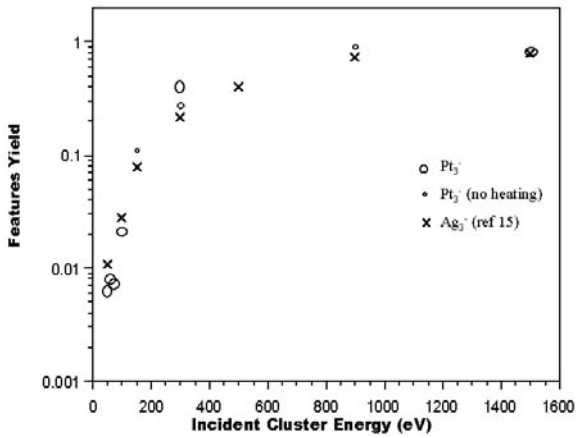

Figure 2. Number of features per incident cluster ion as a function of cluster impact energy. Large circles: Pt_3^- on heated sample. Small circles: Pt_3^- on non-heated sample. Crosses (×): data points for Ag_3^- clusters (from [15]) shown for comparison.

significantly with increasing cluster impact energy, as illustrated by figure 1, in which a graphite sample has been exposed to similar doses of Pt_3^- trimers at three different incident energies, 25 eV, 250 eV and 1 keV. Note that the typical size of the observed features, or 'bumps', is 2–3 nm. Figure 2 shows a plot of the number of features per incident Pt_3^- cluster as a function of the cluster energy and compares these results with previous results for Ag_3^- cluster impact on graphite [15]. We reproduced some of the previous Ag_3^- results at 300 eV, 900 eV and 1500 eV in order to validate the comparison of the two curves. Note also that data points obtained for Pt_3^- deposition on both pre-heated and unheated graphite samples lie on the same curve, see figure 2. Figure 2 shows that the number of features per incident cluster tends towards unity as the cluster energy increases and, moreover, that the Pt_3^- and Ag_3^- curves are more or less identical. We thus obtain the empirical result that the number of features observed in STM depends only on the cluster impact energy and not on the cluster mass for impact energies above 50 eV.

The shape of the curve in figure 2, representing the number of features imaged in STM per incident cluster as a function of incident cluster energy, can be explained [15] in the following way. Pt_3^- (or Ag_3^-) clusters incident at low energy do not penetrate, or 'pin to' the graphite surface; instead they diffuse and aggregate to form a much smaller number of large (∼10–15 nm) particles [6]. The STM images obtained at higher impact energies are then dominated by the results of cluster implantation, leading to plastic deformation of the graphite surface layer [9–11, 15], e.g. deformation above an interstitial C atom displaced by the energetic cluster impact [18, 19]. Also evident from figure 2 is that the probability of creating such a ('visible') feature depends on the cluster energy and not the cluster mass.

Consideration of recent studies of the pinning [13] and implantation of silver clusters in the size range $N = 50$–200 atoms leads us to distinguish two different types of behaviour. The pinning results indicated a pinning threshold associated with the transfer of a critical amount of energy, ∼4.6 eV, to a surface carbon atom. The cluster impact energy (i.e. the experimental pinning threshold) required to transfer this energy scaled linearly with cluster size, and thus mass, as consistent with a binary elastic collision between two quasi-free particles (the massive cluster and the light surface carbon atom). By contrast, molecular dynamics simulations of the implantation of similar size ($N = 20$–200) clusters into the graphite substrate yielded

an implantation depth which did not depend explicitly on cluster mass [12], consistent with the transfer of a fixed energy to each displaced C atom irrespective of cluster mass, and thus violating the simple binary elastic collision model in the implantation regime. While a simple analytical model of the nature of the cluster–carbon collision remains to be developed in this latter case (and would be most valuable), what we can say is that the similarity between the behaviour of Pt_3^- and Ag_3^- clusters in the present study seems then to be consistent with the previous implantation, rather than pinning, results. In particular, the STM images are dominated by cluster implantation. We speculate that Pt_3^- clusters which are (just) pinned to the graphite surface do not present such significant features in the type of 'survey' STM images employed to obtain good statistics.

In summary, we have explored, via STM images obtained over the cluster energy range 50 eV to 1.5 keV, the impact of energetic Pt_3^- and Ag_3^- clusters on the graphite surface. The number of observed features per incident cluster rises with increasing energy through more than two orders of magnitude to a saturation value of 1. The curves for Ag_3^- and Pt_3^- can be overlaid indicating that the process explored is independent of cluster mass, thus violating the binary elastic collision model in the implantation regime. This is consistent with recent molecular dynamics simulations of the implantation (as opposed to pinning) of larger Ag clusters. In future, high resolution STM studies of small pinned clusters on graphite would clearly be of interest, as would studies of the thermal stability of the structures produced.

Acknowledgments

We thank the EPSRC, the School of Physics and Astronomy at the University of Birmingham and Johnson Matthey for financial support of this work.

References

[1] For instance,
Perez A *et al* 1997 *J. Phys. D: Appl. Phys.* **30** 709
[2] Harbich W 2000 *Metal Clusters at Surfaces: Structure, Quantum Properties, Physical Chemistry (Springer Series in in Cluster Physics)* ed K-H Meiwes-Broer (Berlin: Springer) chap. 4
[3] Jensen P 1999 *Rev. Mod. Phys.* **71** 1695
[4] Brechignac C, Cahuzac P, Carlier F, de Frutos M, Masson A, Colliex C, Mory C and Yoon B 1997 *Z. Phys.* **40** 516
[5] Francis G M, Kuipers L, Cleaver J R and Palmer R E 1996 *J. Appl. Phys.* **79** 2942
Francis G M, Goldby I M, Kuipers L, von Issendorff B and Palmer R E 1996 *J. Chem. Soc.* **1** 665
[6] Goldby I M, Kuipers L, von Issendorff B and Palmer R E 1996 *Appl. Phys. Lett.* **69** 2819
[7] Yamaguchi W, Yoshimura K, Tai Y, Maruyama Y, Igarashi K, Tanemura S and Murakami J 2000 *J. Chem. Phys.* **112** 9961
[8] Hall S G, Nielsen M B and Palmer R E 1998 *J. Appl. Phys.* **83** 733
[9] Reimann C T, Andersson S, Brühwiler P, Mårtensson N, Olson L, Erlandsson R, Henkel M and Urbassek H M 1998 *Nucl. Instrum. Methods* B **140** 159
[10] Kaiser B, Bernhardt T M and Rademann K 1998 *Applied. Phys.* **66** S711
[11] Bräuchle G, Richard-Schneider S, Illig D, Beck R D, Schreiber H and Kappes M 1996 *Nucl. Instrum. Methods B* **112** 105
[12] Carroll S J, Nellist P D, Palmer R E, Hobday S and Smith R 2000 *Phys. Rev. Lett.* **84** 2654
[13] Carroll S J, Pratontep S, Streun M, Palmer R E, Hobday S and Smith R 2000 *J. Chem. Phys.* **113** 7723
[14] Aoki T, Seki T, Matsuo J, Insepov Z and Yamada I 1999 *Nucl. Instrum. Methods B* **153** 264
[15] Carroll S J, Hall S G, Palmer R E and Smith R 1998 *Phys. Rev. Lett.* **81** 3715
[16] Henkel M and Urbassek M H 1996 *Nucl. Instrum. Methods* B **112** 105
[17] Hall S G, Nielsen M B, Robinson A W and Palmer R E 1997 *Rev. Sci. Instrum.* **68** 3335
[18] Webb R P, Smith R, Chakarov I, Beardmore K 1996 *Nucl. Instrum. Methods* B **112** 99
[19] Nordlund K, Keinonen J and Mattila T 1996 *Phys. Rev. Lett.* **77** 699